THE ANALYSIS OF PERMANENT DEFORMATIONS OF REPEATEDLY LOADED GRAVELS FROM THE MURA REGION

GREGOR FICKO and BOJAN ŽLENDER

About the authors

Gregor Ficko
Ministry for Transport, Republic of Slovenia
Langusova 4, 1000 Ljubljana, Slovenia
E-mail: gregor.ficko@gov.si

Bojan Žlender
University of Maribor,
Faculty of Civil Engineering
Smetanova ulica 17, 2000 Maribor, Slovenia
E-mail: bojan.zlender@uni-mb.si

Abstract

This contribution presents the results of the analysis of permanent deformations of gravel in the Mura region under repeated loading. The purpose of the analysis is to forecast the development of permanent normalised axial deformations $\varepsilon_1^{p^*}$ regarding the number of loading cycles N and appurtenant stress states during cycling loading. The analysis used the results of tests performed by ZAG Ljubljana and Faculty of Civil Engineering and Geodesy (FGG) of the University of Ljubljana [1]. The analysis considers five types of stone materials of different quantity of crushed grains in the mixture and of different water contents. Four types of stone materials are mixtures of different portions of crushed grains larger than 2 mm (D_{cr} = 87.7 %, 58.9 %, 32.6 % in 0 %), and of the water content around $w = w_{opt}$ - 2%. The stone material with portions of crushed grains larger than 2 mm D_{cr} = 58.9 % is analysed also for water content $w = w_{opt}$ + 0.7 %.
The results of the analysis are deformations expressed as a function of the number of loading cycles N, and a spherical component of the repeated loading p and a distortional component of the repeated loading q. The results can be presented as deformation surfaces in the $\varepsilon_1^{p^*}$ - p - q space for an arbitrary number of cycles N. The relation between the spherical stress component p and the distortional stress component q, at arbitrary values of axial permanent deformations $\varepsilon_1^{p^*}$, gives a failure envelope, and the so called deformation envelopes in the p – q space. The failure envelopes and deformation envelopes are given separately for five types of stone material. The deformation envelopes are low at small values of the axial permanent deformation $\varepsilon_1^{p^*}$. When permanent axial deformations grow, the permanent deformation approaches the failure envelopes. The failure envelopes for individual types of stone material agree with research results performed by [1].
The analysis of permanent deformations also shows their dependence on the portion of crushed material D_{cr} in the mixture of crushed and uncrushed stone material. The deformation envelope for uncrushed stone material is situated in the lowest position, regarding the portion of crushed material in the mixture. With an increased portion of crushed material in the mixture of crushed and uncrushed stone material, the deformation envelope is also higher, similarly to the lawfulness of failure envelopes. The relation of failure and deformation envelopes is mathematically established as a function of the portion of crushed grains larger than 2 mm.
The comparison of stone material results for different water contents shows that a minimal increase of water content above the optimal one essentially increases deformation.

Keywords

Mura region gravel, repeated load triaxial test, granular base material, permanent deformation, normalized axial permanent deformation

1 INTRODUCTION

The construction programme of contemporary four lane roads in the Republic of Slovenia includes the construction of a four-lane highway from Maribor to the Slovenian – Hungarian border. The total length of the highway is 84 km, and the foreseen construction deadline is year 2008. This means that the needs for qualitative natural or recast gravel materials will distinctively grow in the given three year period in the Pomurje region. This material represents more than 90% of materials that comprise the pavement structure.

The designed highway crosses two areas of different geological ground structure. In the first part of lay-out, between Lenart and the river Mura, the highway crosses Slovenske Gorice, a rather hilly region. The ground mostly consists of clay and marley layers, suitable gravel materials can only be found at the river basin of the river Mura. In the second part of lay-out, from the river Mura to the Slovenian – Hungarian border, the highway crosses the river basin of the river Mura, with a very high ground water level, and with under the layers of sandy clays suitable gravel materials placed.

Pomurje is a region characterised by distinctive deficiency of suitable gravel materials for road construction, with respect to quantitative and qualitative criteria. The last analyses of material needs showed that 6.8 to 8.5 million m^3 of natural materials would be needed for the construction of the highway sections from Pesnica to the Slovenian – Hungarian border. The 2.5 million m^3 of the above materials will be incorporated in unbounded and bounded bearing layers, and 4.3 to 6.0 million m^3 will be incorporated in embankments and base course.

One of the key problems of the foreseen highway is how to ensure suitable gravel materials that will fulfil technical and economical criteria of the investment. Therefore, several investigations were done in the past that considered supplies, quality and applicability of natural gravel materials from the Pomurje deposits.

This article presents the analysis of permanent deformations of the Mura region gravel, based on the repeated load triaxial test that simulates traffic loading. The purpose of the analysis is to forecast permanent deformations of the Mura region gravel depending on the number of loading cycles and stress conditions.

The investigation is based on the test results obtained in research projects performed by ZAG and FGG Ljubljana [1] for the investor DARS. In ZAG, repeated load triaxial tests of the Mura region gravel were performed. The variables in research were grain size distribution, density, water content and portion of crushed Mura gravel grains, and repeated loading conditions (static stress, and spherical and distortional stress components).

This paper focuses on the analysis of permanent deformations according to the stress state p - q and the quantity of crushed grains in gravel. The data were taken from the report ZAG, FGG [1] and the master thesis by Ficko [2].

2 THEORETICAL BASIS

The determination of permanent deformations of natural gravel materials from the Pomurje deposits is based on repeated load tests defined in the standards NF P98-235-1 [3] and SIST EN 13286-7 [4] respectively which differ in some respect.

The magnitude and development of permanent deformations depend on static stress state of the material, magnitude of repeated load, magnitude of spherical and distortional repeated load component and the relationship between them, the number of loading cycles, and physical properties of material (density, water content, etc).

The relation between axial permanent deformations $\varepsilon_1^p(N)$ and the number of loading cycles N is given by

$$\varepsilon_1^p(N) = \varepsilon_1^{p^*}(N) + \varepsilon_1^p(100) \qquad (1)$$

where

$\varepsilon_1^p(100)$ is axial permanent deformation after 100 cycles
$\varepsilon_1^{p^*}(N)$ is normalised axial permanent deformation at $N > 100$.

Normalised axial permanent deformation is given by

$$\varepsilon_1^{p^*} = A \cdot \left[1 - \left(\frac{N}{100}\right)^{-B}\right] \qquad (2)$$

where A and B are regression parameters that define deformation growth with the number of loading cycles. The parameter A denotes the limit of the function of permanent axial deformations, whilst the parameter B denotes its deflection.

Fig. 1 presents the numerical solution of the axial permanent deformation ε_1^p and the normalized axial permanent deformation $\varepsilon_1^{p^*}$, for identical gravel material D_{cr} = 58.9% of different water content.

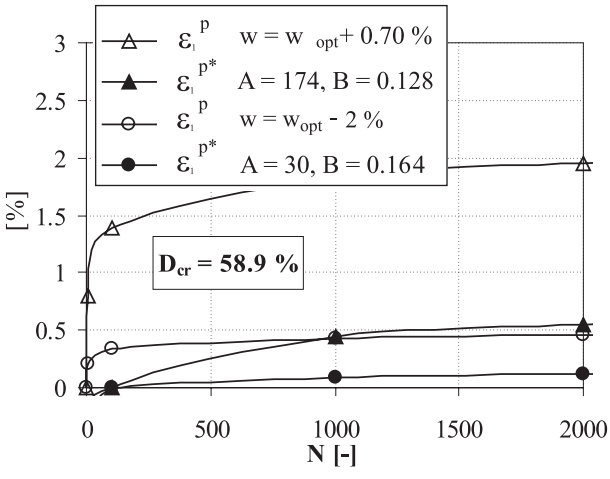

Figure 1. Axial permanent deformation ε_1 and the normalized axial permanent deformation $\varepsilon_1^{p^*}$ vs. the number of loading cycles *N*.

Fig. 2 presents the numerical solution of changes of the axial permanent deformation ε_1 and the normalized axial permanent deformation $\varepsilon_1^{p^*}$ as a function of the number of loading cycles, for identical gravel material D_{cr} = 58.9%, of different water content.

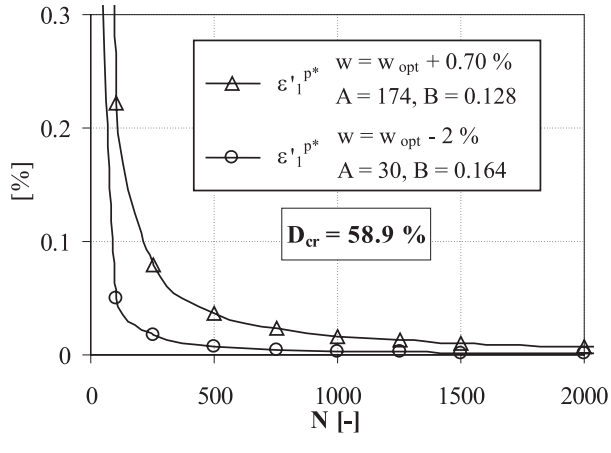

Figure 2. Changes of the axial permanent deformation ε_1 and the normalized axial permanent deformation $\varepsilon_1^{p^*}$ vs. the number of loading cycles *N*.

Changes of the axial permanent deformation ε_1 and the normalized axial permanent deformation $\varepsilon_1^{p^*}$ are given as a function of the number of loading cycles *N* in the following form

$$\frac{d\varepsilon_1^p}{dN} = \frac{d\varepsilon_1^{p^*}}{dN} = \frac{A \cdot B}{N} \cdot \left(\frac{N}{100}\right)^{-B} \qquad (3)$$

The magnitude of the parameters *A* and *B* depend on the stress level that is expressed by spherical and distortional stress components

$$p = \sigma_0 + \frac{\sigma_1 + 2 \cdot \sigma_3}{3} \qquad q = \sigma_1 - \sigma_3 \qquad (4)$$

The maximum axial permanent deformation or the parameter *A* respectively varies with the proportion of maximum distortional and spherical stresses given in Eq. 4

$$A = \frac{\frac{q_{max}}{(p_{max} + p^*)}}{a - b \cdot \frac{q_{max}}{(p_{max} + p^*)}} \qquad (5)$$

where the stress parameter p^* is defined with the section point of the failure line with *q* axis in the *p* - *q* space. It is determined from the linear equation of the test data, according to the method of least square deviation.

$$q = k \cdot p - p^* \qquad (6)$$

where *k* is the slope of the line (Figs. 7 and 8). The parameters *a* and *b* are determined from the test data, with the linear equation of the inverse value of the parameter *A*, using the method of least square deviation (Fig. 6).

$$A^{-1} = a \cdot \left[\frac{q_{max}}{(p_{max} + p^*)}\right]^{-1} - b \qquad (7)$$

The relation between the parameters *a* and *b* gives the slope of the failure line, given by the parameter *M*

$$M = \frac{a}{b} \qquad (8)$$

The value of the failure line at *p*=0 is

$$S = p^* \cdot M \qquad (9)$$

The parameters *M* and *S* define the failure line in the *p* - *q* space

$$q = M \cdot p + S \qquad (10)$$

Equations 5 – 10 are defined in [3].

Development of permanent axial deformations (Eq.2) can also be given in the *p* - *q* space by

$$\varepsilon_1^{p^*}(N, p, q) = \varepsilon_1^{p^*}(N, p_0, q_0) \cdot f(p) \cdot f(q) \qquad (11)$$

where the characteristic value of the permanent axial deformation ε_0 is given at selected values of the spherical stress component p_0 and the distortional stress component q_0

$$\varepsilon_0 = \varepsilon_1^{p^*}(N, p_0, q_0) \qquad (12)$$

The magnitude of permanent axial deformation depends on the spherical stress component p and the distortional stress component q, following the exponential equation

$$\varepsilon_1^{p^*}(N,p,q) = \varepsilon_0 \cdot e^{A\left(1-\left(\frac{p}{p_0}\right)^B\right)} \cdot e^{-C\left(1-\left(\frac{q}{q_0}\right)^D\right)} \qquad (13)$$

where A and B are parameters that define variation of the normalized permanent axial deformation $\varepsilon_1^{p^*}$ as a function of the spherical stress component p, C and D are parameters that define variation of permanent axial deformation as a function of the distortional stress component q.

Similarly, the variation of other influences (density, water content) can be written. Due to minimal changes of these parameters for individual types of material they will be considered as a constant condition. From Eq. 12 the normalized permanent axial deformation $\varepsilon_1^{p^*}$ is expressed considering the spherical stress component p and the distortional stress component q, which can be given with the surface in the $\varepsilon_1^{p^*}$ - p - q space.

At a certain constant value of the spherical stress component p, the value of $\varepsilon_1^{p^*}$ increases exponentially with the increased q, and at a certain limit value q diverges.

For each plane in the $\varepsilon_1^{p^*}$ - p - q space at an arbitrary value of p, the relation between the distortional stress component q and the normalized permanent axial deformation $\varepsilon_1^{p^*}$ can be determined using Eq. 12

$$q(\varepsilon_1^{p^*}) = q_0 \cdot \left[1 + \frac{1}{C} \cdot \ln\left(\frac{1}{k_p}\frac{\varepsilon_1^{p^*}}{\varepsilon_0}\right)\right]^{1/D} \qquad (14)$$

where the parameter k_p is given by

$$k_p = e^{A\left(1-\left(\frac{p}{p_0}\right)^B\right)} \qquad (15)$$

With an increased value of the spherical stress component p and a certain constant value of the distortional stress component q, the value of $\varepsilon_1^{p^*}$ converges to a certain value.

For each plane in the $\varepsilon_1^{p^*}$ - p - q space at an arbitrary value of the q relation between the spherical stress component p and the normalized permanent axial deformation $\varepsilon_1^{p^*}$ can be determined using Eq. 12

$$p(\varepsilon_1^{p^*}) = p_0 \cdot \left[1 - \frac{1}{A} \cdot \ln\left(\frac{1}{k_q}\frac{\varepsilon_1^{p^*}}{\varepsilon_0}\right)\right]^{1/B} \qquad (16)$$

where the parameter k_q is given by

$$k_q = e^{-C\left(1-\left(\frac{q}{q_0}\right)^D\right)} \qquad (17)$$

From Eq. 13 the failure line and the deformation line in the p - q space can be determined at a certain number of loading cycles N.

3 GRAVEL FROM THE MURA REGION

The investigation of natural gravel quality from the existent deposits in the Pomurje region (to be used in individual pavement layers) comprised:

- laboratory research of primary rock,
- laboratory research of individual grain composition of granular aggregate after crushing primary rock,
- laboratory research of grain mixture of granular aggregate produced in separations,
- field research of the unbounded bearing layers quality of the pavement structure in individual test fields.

The investigations of stone material quality were done in laboratories and in field in Pomurje (see the reports of Igmat [5] and ZAG [6]), dynamic triaxial tests were performed in the laboratory of ZAG (see the report [1]).

All laboratory investigations were performed within the research project of ZAG [7]. They comprise:

a. Properties of stone materials
   - mineralogical properties (mineralogical and petrographical composition of rocks, content of hazardous admixtures),
   - space and mechanical properties,
   - quality of stone materials,
   - physical properties (density, grain size distribution, water contents),
   - geometrical properties of stone grain mixture,
   - mechanical properties of stone grain mixture

b. Experimental incorporation of stone grain mixture
   - in the laboratory,
   - in field

c. Procedures for improving the incorporation of stone grain mixture, such as
   - crushing,
   - improvement with alloys (electro filter ash),
   - soil reinforcement using geotextile or geogrid

d. Repeated load triaxial tests

The performance of laboratory investigations of properties and quality of natural stone materials, and the research results are presented in detail in the reports [5], [6] and [7]. The investigations of stone materials from Pomurje deposits confirmed that the gravel from Mura region is suitable due to quality, applicability and supplies.

The presented analysis uses data from the report [1] and the master thesis of Ficko [2]. The analysis considers five types of stone materials. Four of them were tested with repeated loading at the water content $w = w_{opt}$ - 2%. Stone material of D_{cr} = 58.9% was further tested at the water content $w = w_{opt}$ + 0.7%. Physical properties of four different types of stone materials are given in Table 1.

Table 1. Physical properties of stone materials

Type of stone material	Portion of crushed grains >2 mm D_{cr} [%]	Grain mixture density $\rho_{d,max}$ [g/cm^3]	Optimal water content w_{opt} [%]
Crushed mixture	87.7	2.240	5.51
Crushed plus uncrushed mixture 1:2	58.9	2.266	4.80
Crushed plus uncrushed mixture 1:1	32.6	2.253	3.80
Uncrushed mixture	0	2.248	4.98

Grain size distributions of four considered types of stone materials are shown in Figs. 3 to 6.

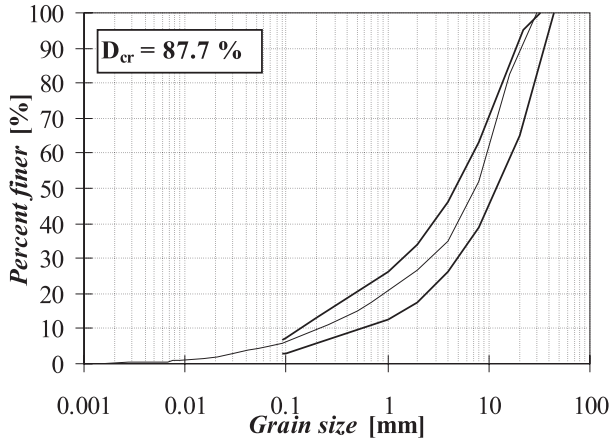

Figure 3. Grain size distribution of crushed Mura region gravel with the portion of crushed grains larger than 2 mm D_{cr}=87.7%

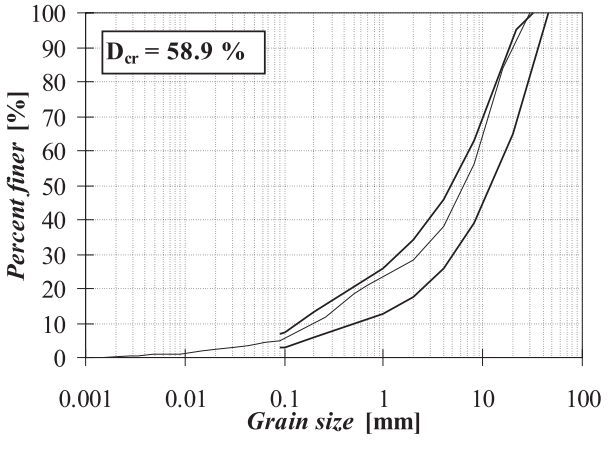

Figure 4. Grain size distribution of mixture of crushed and uncrushed Mura region gravel with the portion of crushed grains larger than 2 mm D_{cr} =58.9%

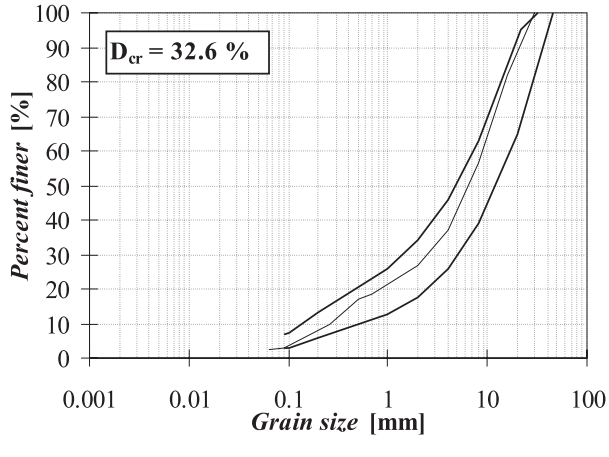

Figure 5. Grain size distribution of mixture of crushed and uncrushed Mura region gravel with the portion of crushed grains larger than 2 mm D_{cr} =32.6%

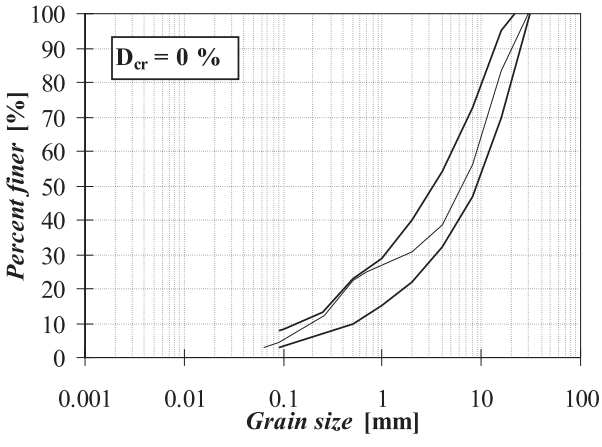

Figure 6. Grain size distribution uncrushed Mura region gravel D_{cr}=0%

4 REPEATED LOAD TRIAXIAL TESTS

In the laboratory of ZAG repeated load triaxial tests of Mura gravel were performed. Dynamic loading following standard and modified procedures [4] was applied in testing.

In the first part of the research the programme of triaxial tests of stone material grain mixture was designed to analyse plastic deformations of the stone grain mixture dependent on the crushed stone grain portion in the mixture. Based on the results of these tests the the lowest admissible portion of crushed stone grains in the unbounded bearing layer was determined, at which the resulting plastic deformations under traffic load would not have any harmful effect on durability and quality of the pavement structure. The second part of the research comprises the analyses of effects produced by alloys. Alloys were added to improve functionality of uncrushed stone material (electro filter ash, geotextile, geogrid). The third part of the research comprises the evaluation of stone grains dynamic properties with a modified triaxial test. This contribution treats the first part of research.

Repeated load triaxial tests were performed on specimens of the water content $w = w_{opt}$ - 2% and $w = w_{opt}$ + 0.7 %. Proctor density of specimens was about 98%. With data acquired through analysis and using Boyce's nonlinear rheological model we determined the relation between number of repeated loading and the development of permanent deformations, and the relation between stresses and permanent deformations. This led us to determining the parameters of the failure line of the studied material.

A set of repeated load triaxial tests in different stress conditions was performed on each type of stone material to establish permanent deformations (see Figs. 7 and 8).

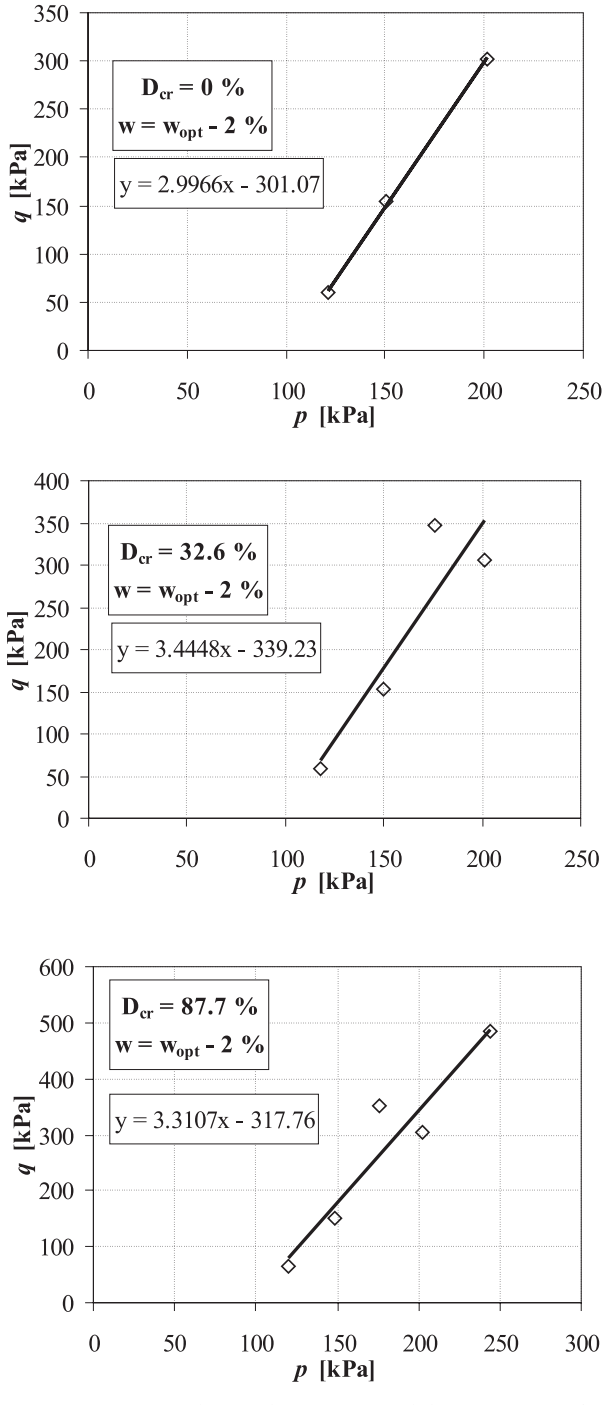

Figure 7. Stress conditions during tests and determination of the initial parameter p^* for different types of stone material at the water content $w = w_{opt}$ - 2%.

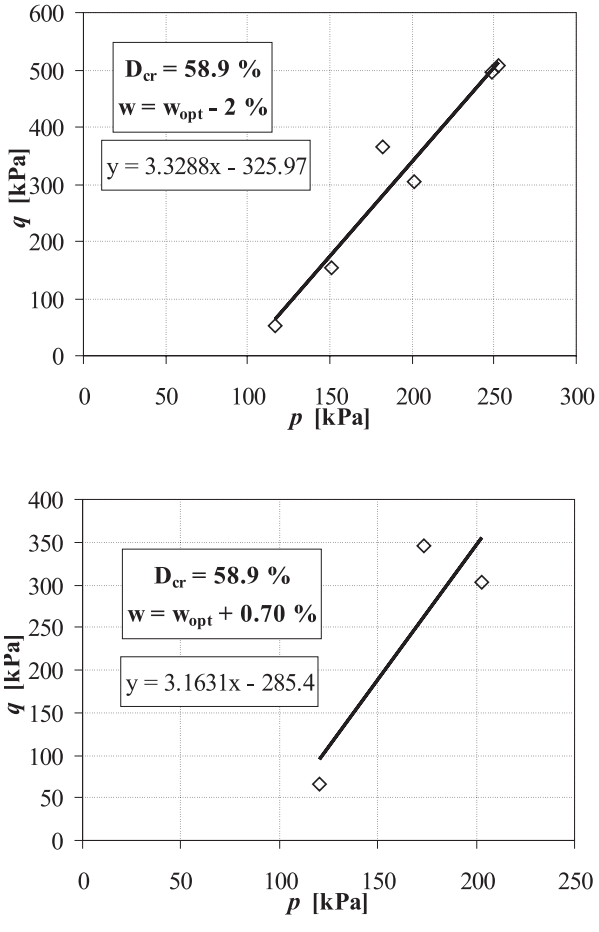

Figure 8. Stress conditions during tests and determination of the initial parameter p^*, for D_{cr} = 58.9, $w = w_{opt}$ - 2% and $w = w_{opt}$ + 0.7%.

5 DEFORMATION ANALYSIS

Deformation analysis was performed on five types of stone material. A set of repeated load triaxial tests was performed on each type of stone material. From Eqs. (1) and (2) the parameters A and B were determined, which define a numerical solution for the development of permanent axial deformations $\varepsilon_1^p(N)$ and normalised permanent axial deformations $\varepsilon_1^{p^*}(N)$. Figs. 1 and 2 show a numerical solution for the course of permanent axial deformations ε_1^p and normalised permanent axial deformations $\varepsilon_1^{p^*}$, and changes regarding the number of loading cycles N for stone material D = 58.9 %, of different water content. The increased water content distinctively influences the magnitude of deformations $\varepsilon_1^p(N)$ and $\varepsilon_1^{p^*}(N)$.

Figs. 9 and 10 show numerical solutions of the normalised axial permanent deformation $\varepsilon_1^{p^*}$ for all material types.

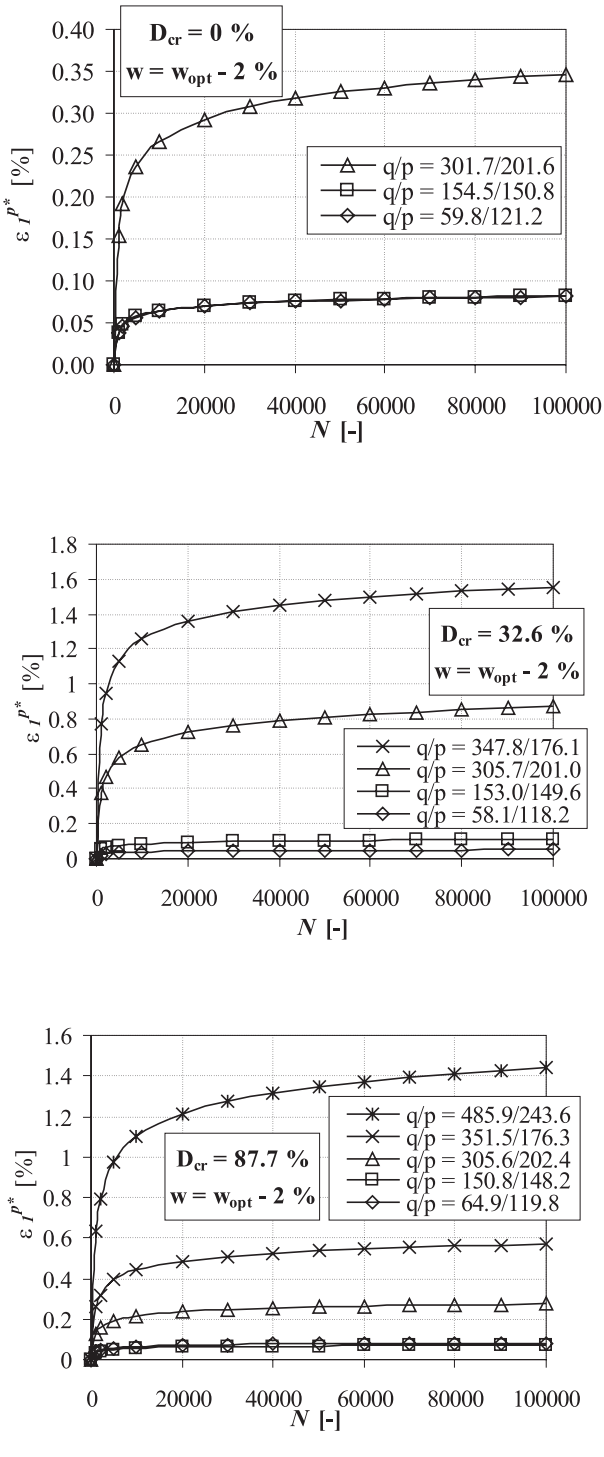

Figure 9. Normalised axial permanent deformation $\varepsilon_1^{p^*}$ vs. the number of loading cycles N for different types of stone materials at water content $w = w_{opt}$ - 2%.

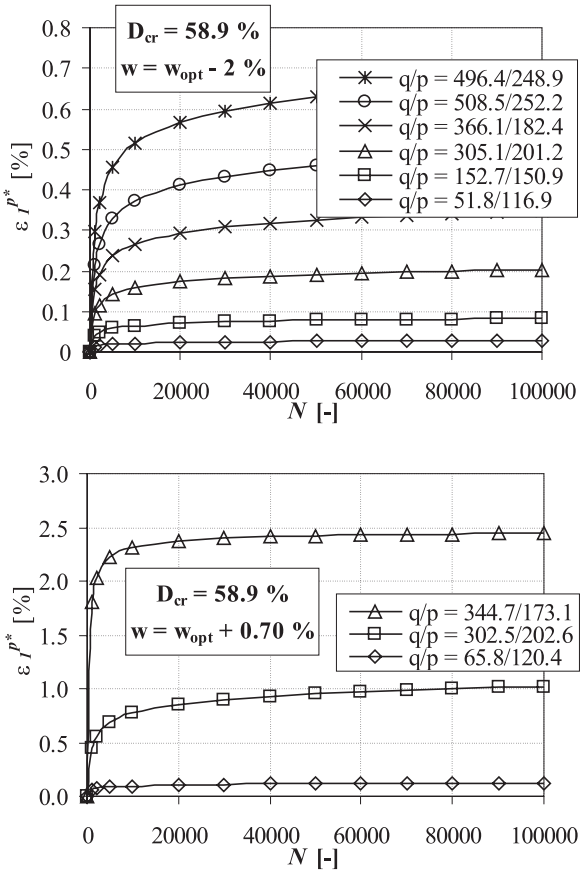

Figure 10. Normalised axial permanent deformation ε_1^{p*} vs. the number of loading cycles N for $w = w_{opt}$ - 2% and $w = w_{opt}$ + 0.7%.

The relation between the spherical stress component p and the distortional stress component q for all tests on individual types of stone material are presented in Figs. 7 and 8.

Fig. 11 shows determination of the initial parameters a and b (Eq. 7). The same approach was applied to all types of stone material.

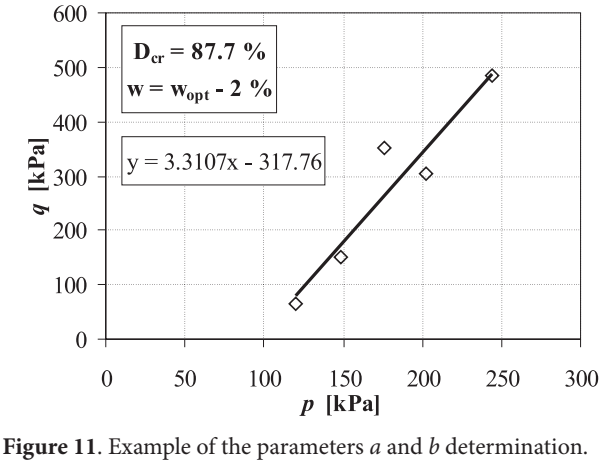

Figure 11. Example of the parameters a and b determination.

Using Eqs. 8 to 10 we obtain failure envelopes in the p – q space for individual types of stone material.

Fig. 12 shows failure envelopes in the p – q space for different mixtures of uncrushed and crushed stone material for D_{cr} = 0 - 87.7 %.

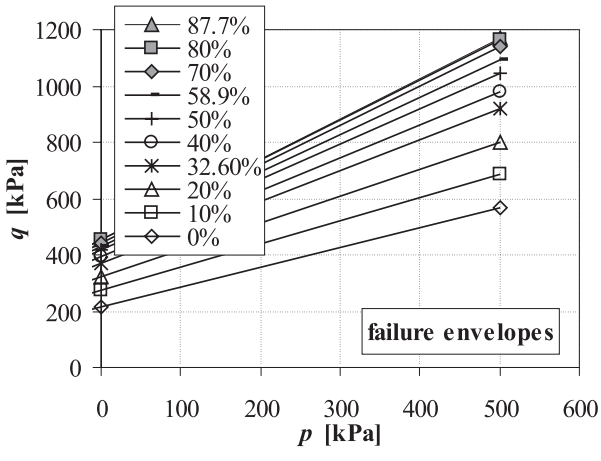

Figure 12. Failure envelopes for different portions of crushed grains, D_{cr} = 0-87.7 %, at water content $w = w_{opt}$ - 2%.

Fig. 13 shows the course of normalised axial permanent deformation ε_1^{p*} as a function of the distortional stress q and the spherical stress p for different types of stone material.

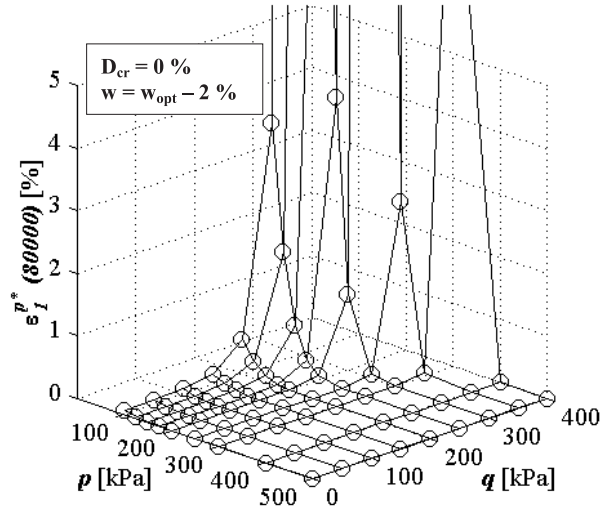

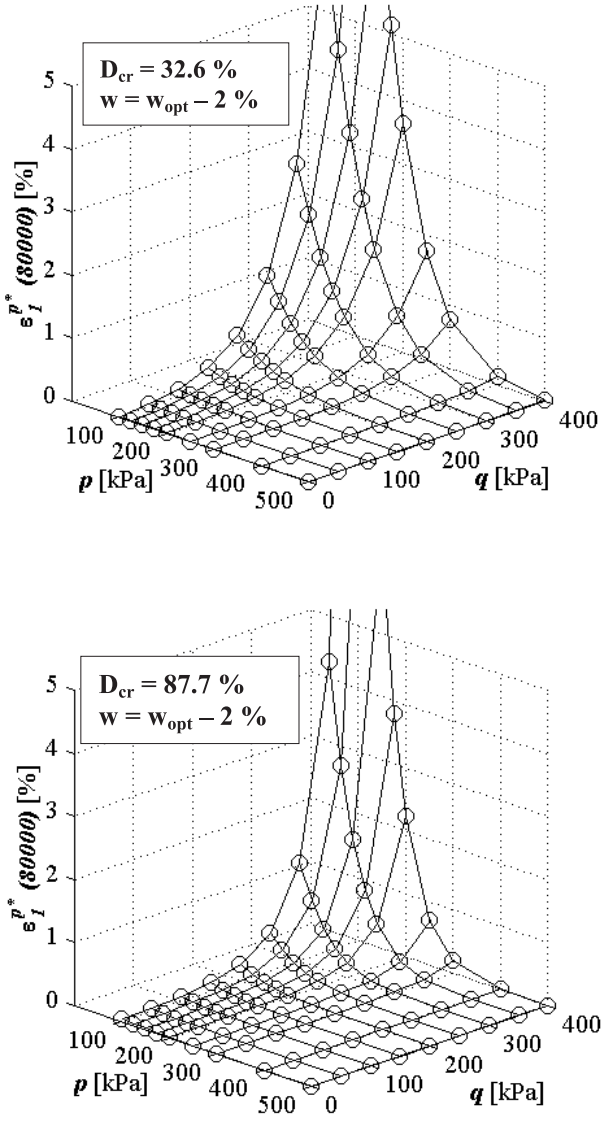

Figure 13. Normalised axial permanent deformation $\varepsilon_1^{p\star}$ in the $\varepsilon_1^{p\star}$ - p – q space for different types of stone material at water content $w = w_{opt}$ - 2%.

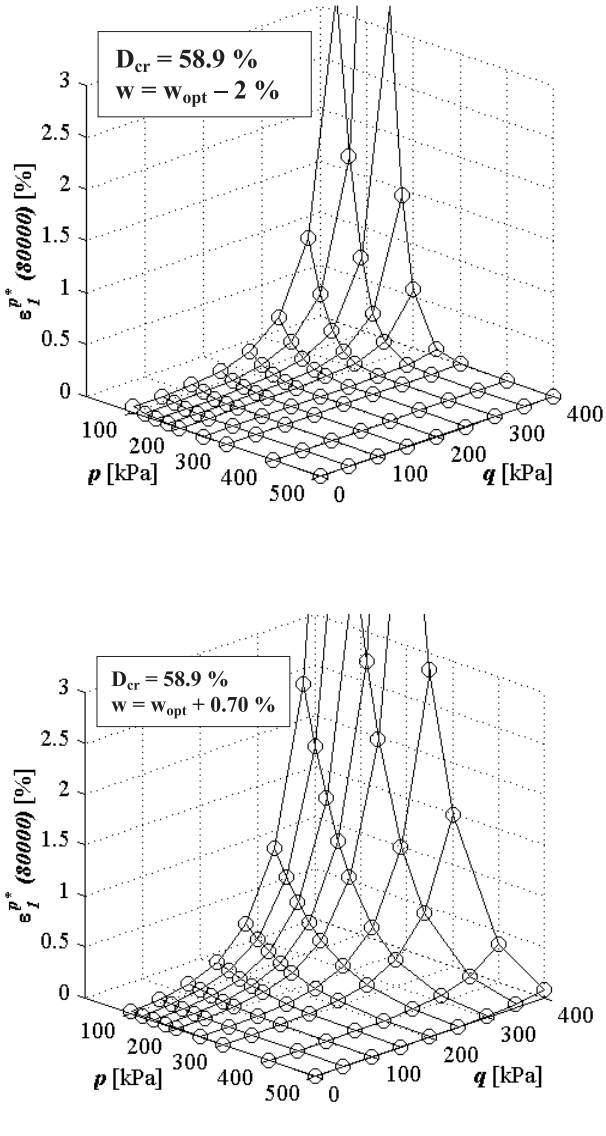

Figure 14. Normalised axial permanent deformation $\varepsilon_1^{p^*}$ in the $\varepsilon_1^{p^*}$ - p – q space for stone material of different water contents.

Fig. 14 shows the course of normalised axial permanent deformation $\varepsilon_1^{p\star}$ as a function of the distortional stress q and the spherical stress p for the stone material D_{cr} = 58.9% for different water contents ($w = w_{opt}$ - 2% in $w = w_{opt}$ + 0.7%).

The relation between the normalised axial permanent deformation $\varepsilon_1^{p^*}$ and the distortional stress q for the constant spherical stress p (view in individual planes in the $\varepsilon_1^{p^*}$ - p – q space) is obtained from Eq. 14. Fig. 15 shows these relations for different types of stone materials.

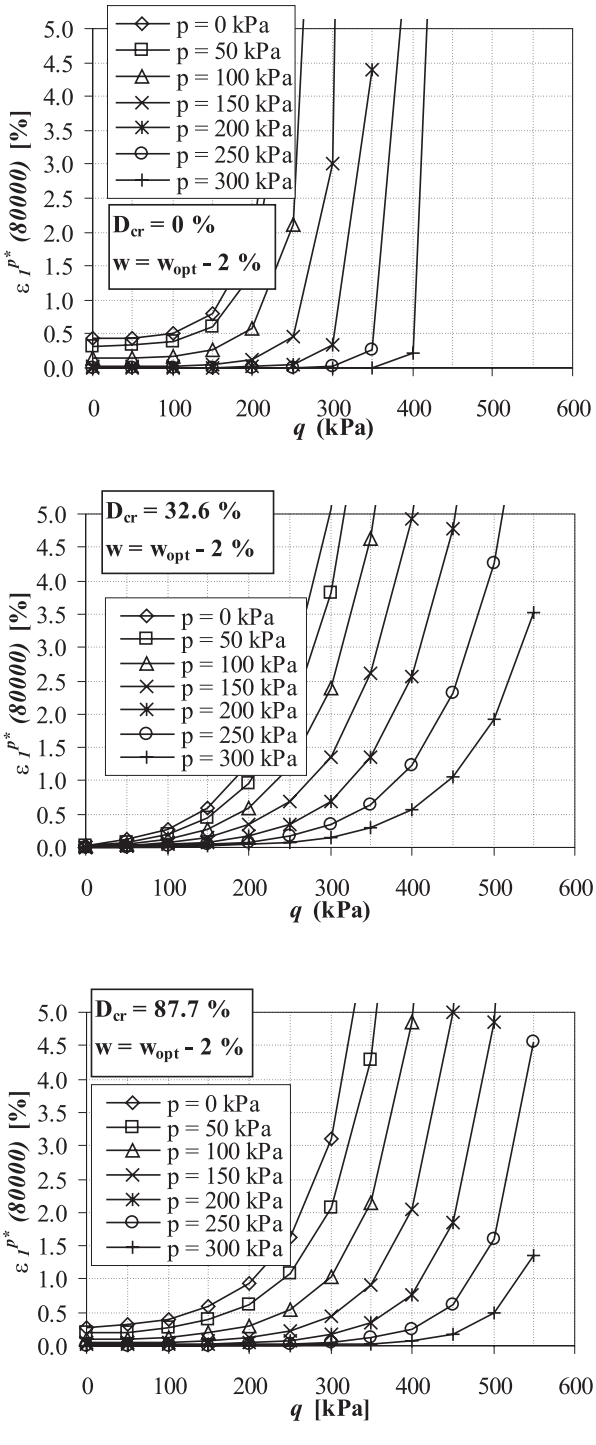

Figure 15. Normalised axial permanent deformation $\varepsilon_1^{p^*}$ vs. the distortional stress q for different constant spherical stresses p and different types of stone material at the water content $w = w_{opt}$ - 2%.

Fig. 16 shows the relation between the normalised axial permanent deformation $\varepsilon_1^{p^*}$ and the distortional stress q for stone material D_{cr} = 58.9% at different water contents $w = w_{opt}$ - 2% and $w = w_{opt}$ + 0.7%.

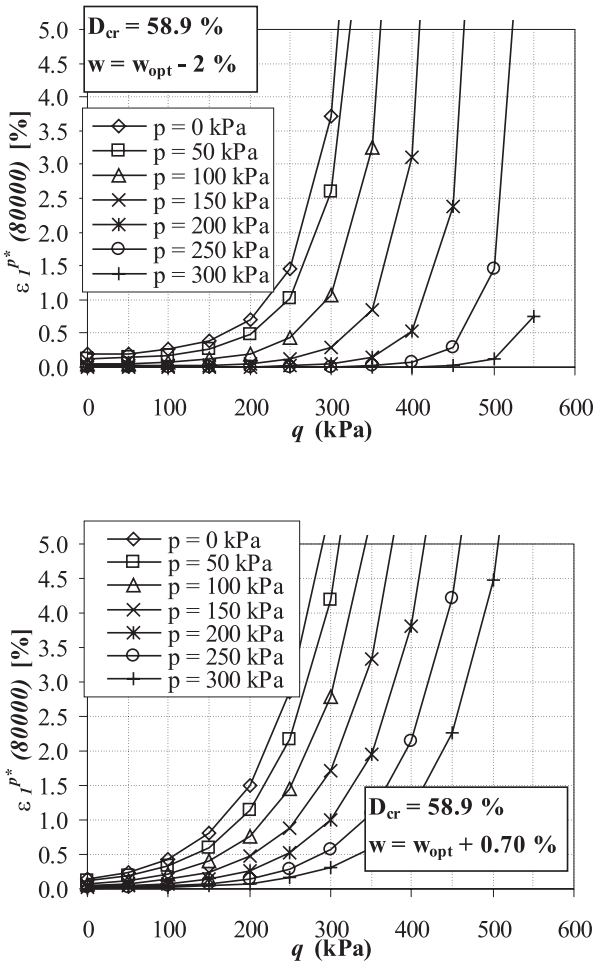

Figure 16. Normalised axial permanent deformation $\varepsilon_1^{p^*}$ vs. the distortional stress q for constant spherical stresses p and stone material D_{cr} = 58.9% at water contents $w = w_{opt}$ - 2% and $w = w_{opt}$ + 0.7%.

The relation between the spherical stress component p and the distortional stress component q at a certain value of the normalised axial permanent deformation $\varepsilon_1^{p^*}$, gives the so called deformation envelopes. Deformational envelopes are low at small values of the normalised axial permanent deformation $\varepsilon_1^{p^*}$. They increase with the increase of permanent axial deformation and approach the failure envelope, which represents a limit state of the relation q/p. Failure envelopes and deformation envelopes are given for five types of stone material. Failure envelopes of different types of stone materials are in agreement with the research results performed by ZAG and FGG [1].

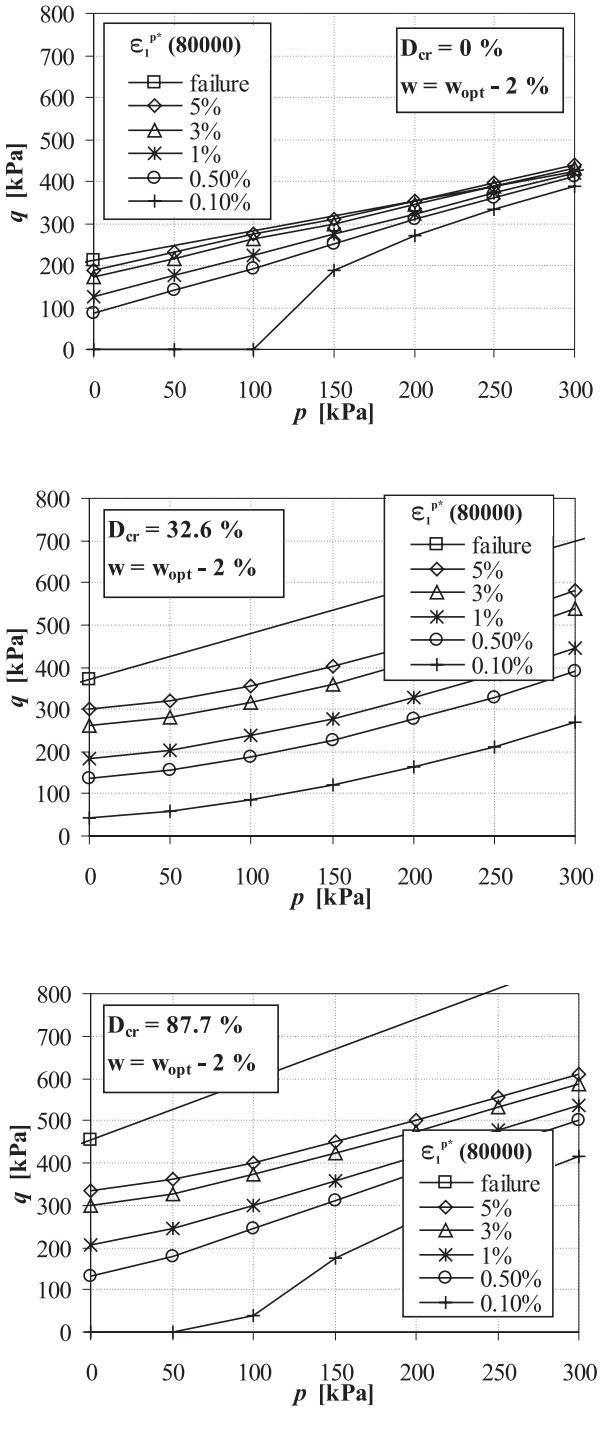

Figure 17. Deformation envelopes for different values of the normalised axial permanent deformation $\varepsilon_1^{p^*}$ for different types of stone material at the water content $w = w_{opt}$ - 2%.

Deformation envelopes are given for all types of stone materials. We can realize that when deformations grow the deformation envelope approaches the failure envelope. At a sufficiently small value of axial permanent deformation (actual to application) the deformation envelope is situated lower than the failure envelope.

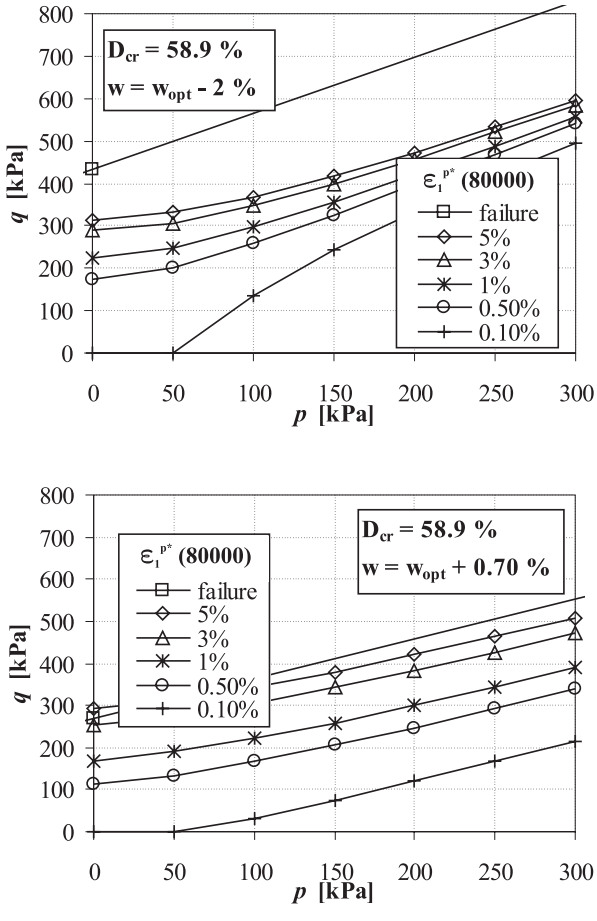

Figure 18. Deformation envelopes for different values of the normalised permanent axial deformation $\varepsilon_1^{p^*}$ and stone material D_{cr} = 58.9% at the water contents $w = w_{opt}$ - 2% and $w = w_{opt}$ + 0.7%.

The deformation envelope for uncrushed stone material is situated at the lowest position, regarding the portion of crushed material in mixture. With the increased portion of crushed material in mixture of crushed and uncrushed stone material the deformation envelope is higher and is in agreement with the results in report ZAG and FGG [1].

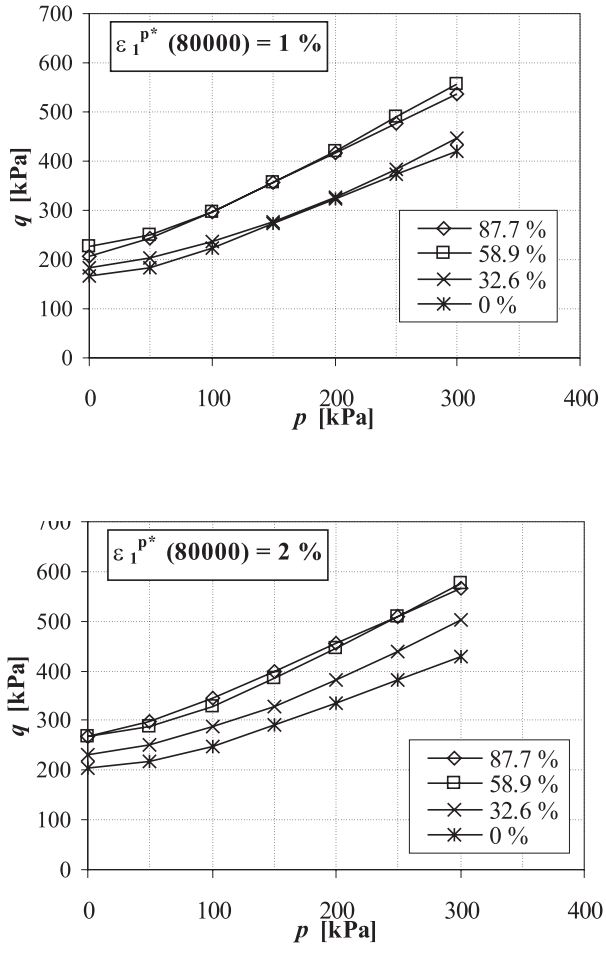

Figure 19. The influence of the crushed material portion D_{cr} on the course of the deformation envelope at the water content $w = w_{opt}$ - 2%.

CONCLUSIONS

The analysis of development of permanent axial deformations of gravel in the Mura region due to repeated loading was performed. The investigation proceeded from the test results obtained within the scope of research project that were made by ZAG and FGG [1].

This contribution is limited to the analysis of development of permanent axial deformations regarding the number of loading cycles N and appurtenant stress states q - p during the repeated loading for different types of stone material. Types of stone material were determined with regard to the quantity of crushed grains in gravel and to water content.

The results of the analysis are deformations expressed as a function of the number of loading cycles N and a spherical component of the repeated loading p and a distortional component of the repeated loading q. The results can be presented as deformation surfaces in the $\varepsilon_1^{p^*}$ - p - q space for an arbitrary number of the cycles N. The relation between the spherical stress component p and the distortional stress component q, at arbitrary values of axial permanent deformations $\varepsilon_1^{p^*}$, gives the so called deformation envelopes and the failure envelope as a limit state. The failure envelopes and deformation envelopes are given for five types of stone material. The failure envelopes for individual types of stone material agree with research results performed by ZAG and FGG [1]. The deformation envelopes are low at small values of the permanent axial deformation $\varepsilon_1^{p^*}$. When permanent axial deformations are growing, the permanent deformation approaches the failure envelopes.

The deformation envelope for uncrushed stone material is situated at the lowest position, regarding the portion of crushed material in the mixture. With an increased portion of crushed material in the mixture of crushed and uncrushed stone material, the deformation envelope is also higher similarly to the lawfulness of failure envelopes.

The comparison of stone material results for different water contents shows that a minimal increase of the water content above the optimal one essentially increases deformation.

REFERENCES

[1] Pavšič P., and Petkovšek A. (2004). The use of Mura region gravel for pavements, final report (in Slovene). ZAG Ljubljana, Faculty of Civil Engineering and Geodesy, University of Ljubljana, Ljubljana.

[2] Ficko, G. (2005). The optimisation of using the granular base material from sites in the Mura region, constructing the Lenart – Pince highway (in Slovene). MSc. Thesis, University of Maribor, Maribor.

[3] NF P98-235-1 (1995). Essais relatifs aux chaussées – Matériaux non traités – Partie 1: essai triaxial à chargements répétés, AFNOR.

[4] SIST EN 13286-7 (2004). European Standard: Unbound and hydraulicaly bound mixtures – Part 7: Repeated load triaxial test for unbound mixtures.

[5] Igmat (2002). Investigation report of separated Mura region gravel (in Slovene). Igmat d.d., Ljubljana.

[6] ZAG (1998). Report on stock, production capacity of plant and quality of gravel in the Mura region (in Slovene). ZAG Ljubljana, Ljubljana.

[7] Petkovšek A. et al. (1999). The usefullness of Mura region gravels for constructing heavy and very heavy traffic loads highways (in Slovene). ZAG Ljubljana, Ljubljana.
[8] Pavšič P., and Lenart S. (2002). Determination of dynamic characteristics for unbound granular materials with cyclic load triaxial test – Slovenian experience. *5. Slovenian Road and Transportation congress, DRC Road and transportation Research Association of Slovenia*, Ljubljana.
[9] Pavšič P., Lenart S., and Petkovšek A. (2004). The permanent deformations of Mura gravel in relationship of percent of crushed particles. *6. Slovenian Road and Transportation congress, DRC Road and transportation Research Association of Slovenia*, Ljubljana.